Published in final edited form as:
J Proteome Res. 2008 July ; 7(7): 2959–2972. doi:10.1021/pr8000892.

Proteomic Expression Analysis of Surgical Human Colorectal Cancer Tissues: Up-Regulation of PSB7, PRDX1, and SRP9 and Hypoxic Adaptation in Cancer

Jung-hyun Rho[†,||], **Shuzhen Qin**[‡,||,#], **Julia Y. Wang**[*,†,||], and **Michael H. A. Roehrl**[*,§,||]
Channing Laboratory, Department of Medicine, Brigham and Women's Hospital, Department of Urology, Brigham and Women's Hospital, Department of Pathology and Laboratory Medicine, Massachusetts General Hospital, Boston, Massachusetts 02115 and Harvard Medical School, Boston, Massachusetts 02114

Abstract

Colorectal adenocarcinoma is one of the worldwide leading causes of cancer deaths. Discovery of specific biomarkers for early detection of cancer progression and the identification of underlying pathogenetic mechanisms are important tasks. Global proteomic approaches have thus far been limited by the large dynamic range of molecule concentrations in tissues and the lack of selective enrichment of the low-abundance proteome. We studied paired cancerous and normal clinical tissue specimens from patients with colorectal adenocarcinomas by heparin affinity fractionation enrichment (HAFE) followed by 2-D PAGE and tandem mass spectrometric (MS/MS) identification. Fifty-six proteins were found to be differentially expressed, of which 32 low-abundance proteins were only detectable after heparin affinity enrichment. MS/MS was used to identify 5 selected differentially expressed proteins as proteasome subunit β type 7 (PSB7), hemoglobin α subunit (HBA), peroxiredoxin-1 (PRDX1), argininosuccinate synthase (ASSY), and signal recognition particle 9 kDa protein (SRP9). This is the first proteomic study detecting the differential expression of these proteins in human colorectal cancer tissue. Several of the proteins are functionally related to tissue hypoxia and hypoxic adaptation. The relative specificities of PSB7, PRDX1, and SRP9 overexpression in colon cancer were investigated by Western blot analysis of patients with colon adenocarcinomas and comparison with a control cohort of patients with lung adenocarcinomas. Furthermore, immunohistochemistry on tissue sections was used to define the specific locations of PSB7, PRDX1, and SRP9 up-regulation within heterogeneous primary human tumor tissue. Overexpression of the three proteins was restricted to the neoplastic cancer cell population within the tumors, demonstrating both cytoplasmic and nuclear localization of PSB7 and predominantly cytoplasmic localization of PRDX1 and SRP9. In summary, we describe heparin affinity

*To whom correspondence should be addressed. Michael H. A. Roehrl, M.D., Ph.D., Department of Pathology and Laboratory Medicine, Massachusetts General Hospital, 55 Fruit Street, Boston, MA 02114. Phone, +1-617-726-2967; fax, +1-617-726-7474; e-mail, E-mail: michael_roehrl@hms.harvard.edu. Julia Y. Wang, Ph.D., Channing Laboratory, Brigham and Women's Hospital, 181 Longwood Avenue, Boston, MA 02115. Phone, +1-617-732-8585; fax, +1-617-731-1541; e-mail, E-mail: julia_wang@rics.bwh.harvard.edu.
[†]Channing Laboratory, Department of Medicine, Brigham and Women's Hospital.
[||]Harvard Medical School.
[#]Current address: Synta Pharmaceuticals, Lexington, MA 02421.
[‡]Department of Urology, Brigham and Women's Hospital.
[§]Department of Pathology and Laboratory Medicine, Massachusetts General Hospital.

Supporting Information Available: Supplementary experimental procedures; supplementary tables of clinical data of the colorectal and lung adenocarcinoma samples included in this study, and detailed information on the MS/MS sequencing of the five identified protein spots; supplementary figures of representative image pairs showing 2-D PAGE analyses of tissue protein extracts from normal colonic mucosa or adeno-carcinoma, detectability and heparin affinity characteristics of the 56 identified differentially expressed protein spots, and validation of SRP9 overexpression by Western blotting. This material is available free of charge via the Internet at http://pubs.acs.org.

fractionation enrichment (HAFE) as a prefractionation tool for the study of the human primary tissue proteome and the discovery of PSB7, PRDX1, and SRP9 up-regulation as candidate biomarkers of colon cancer.

Keywords

Colorectal carcinoma; low-abundance proteome; heparin affinity fractionation enrichment; two-dimensional gel electrophoresis; mass spectrometry; immunohistochemistry; proteasome subunit β type 7; peroxiredoxin-1; signal recognition particle 9 kDa protein; hypoxic adaptation

Introduction

Colorectal cancer accounts for 13–14% of clinical cancer presentations and 10–13% of overall cancer mortality, which makes it one of the most prevalent and deadly cancers worldwide.[1] Colorectal adenocarcinoma arises most frequently from preneoplastic polypoid adenomas through a sequence of progressively malignant stages. Currently, clinical detection methods for colorectal cancer include biennial fecal occult blood tests and regular sigmoidoscopies or colonoscopies on selected patients. Carcinoembryonic antigen (CEA) is a blood-based protein biomarker that is in clinical use for postsurgical detection of recurrence and monitoring of metastatic disease burden.[2,3] However, CEA is neither sensitive nor specific enough for diagnosis or early detection of the disease.

Recently, it has been recognized that the large dynamic range of tissue protein concentrations (spanning 10^5–10^{12}-fold differences) poses a formidable challenge to proteomic discovery. Consequently, the rich low-abundance proteome, while functionally very much of critical importance, has thus far largely eluded investigation in favor of relatively few high-abundance components, such as structural or cytoskeletal proteins. For example, proteomic profiling by 2-D PAGE or nongel-based approaches (e.g., MS/MS) can be expected to have missed low-abundance proteins and may have provided an incomplete picture because the individual dynamic range of these methods is at best 3 to 5 orders of magnitude. One approach to address this situation is to apply targeted prefractionation techniques prior to proteomic analysis in order to specifically enrich for the low-abundance proteome while removing unwanted abundant proteins.[4–7]

In our present study, we chose heparin affinity chromatography as a prefractionation tool for human colorectal cancer tissue proteins isolated from primary surgical specimens. Heparin is a member of the glycosaminoglycan family and consists of variably sulfated repeating disaccharide units. Heparin has two main modes of interaction with proteins.[5,6] First, heparin can function as a specific affinity ligand, for example, in its interaction with components of the blood coagulation cascade or extracellular growth factors. Second, due to its sulfate groups and polyanionic nature, heparin can serve as a high capacity cation exchanger and bind a broad variety of proteins with a range of affinities. Furthermore, the interactions of heparin with various proteins *in vivo* may have significant physiologic implications in cancer and other diseases. Hence, binding of heparin, via a combination of specific affinity association and nonspecific electrostatic ion pairing, may be a powerful tool for the selection and enrichment of low-abundance proteins as potential cancer biomarkers.

In our study, we investigated heparin affinity fractionation enrichment (HAFE) of human colonic tissue proteins. Using a computational 2-D Difference Gel Electrophoresis (DIGE) comparison, we found that the proteomic profiles of heparin-binding fractions differed from those of unfractionated total protein extracts. While previously abundant proteins were relatively depleted, many low-abundance proteins were enriched and newly visible in heparin-

binding fractions. We then applied our HAFE technique to matched pairs of colon adenocarcinoma and normal tissue specimens from patients who had undergone surgical colectomy procedures. Our subsequent 2-D PAGE comparison identified 56 differentially expressed proteins, 5 of which were selected for further study because of their favorable 2-D electrophoretic separation behavior (clear spot separation without overlap). The identities of these proteins were unambiguously established by mass spectrometric sequencing. Interestingly, none of the proteins have thus far been implicated in colon carcinogenesis. Therefore, these proteins may represent new candidate biomarkers of disease. Subsequently, we focused on three particular proteins, that is, PSB7, PRDX1, and SRP9, for further study because their functional context was particularly appealing. In our initial 2-D HAFE-PAGE experiments, these proteins were found to be up-regulated in cancer tissue. Quantitative analysis of PSB7, PRDX1, and SRP9 proteins in an independent prospective set of patients with colon carcinomas confirmed their increased abundance in cancer. For comparison, we also examined the levels of PSB7, PRDX1, and SRP9 protein expression in a control cohort of pulmonary adenocarcinomas.

Human cancer tissue is a complicated, highly heterogeneous composite, typically including an admixture of *bona fide* neoplastic cancer cells, benign epithelial elements, mesenchymal stromal cells, blood and lymphatic vessels, nerve tissue, intercellular matrix elements, areas of necrosis or apoptosis, and numerous other components. By immunohistochemical techniques, overexpression of PSB7 was found in both cytoplasmic and nuclear compartments of the neoplastic colon cancer cells, while PRDX1 and SRP9 overexpression was confined to the cytoplasmic compartment.

In sum, we describe the discovery of PSB7, PRDX1, and SRP9 up-regulation in human colon adenocarcinomas using a pre-fractionation approach that facilitates investigation of the tissue proteomes of primary human surgical specimens.

Experimental Procedures

Clinical Tissue Specimen Collection

Ten matched pairs of colon adenocarcinomas and adjacent normal colonic mucosa and 15 matched pairs of lung adenocarcinomas and adjacent normal lung tissue were collected at the Department of Pathology and Laboratory Medicine, Massachusetts General Hospital, Boston, MA. Fresh tissue samples were dissected in the Frozen Section Laboratory immediately after surgical removal of the specimen from the patient and carefully snap-frozen in liquid nitrogen. The frozen samples were stored at −80 °C until further analysis. Routine diagnostic tissue was fixed in formalin and embedded in paraffin. A summary of the tissue samples is shown in Supplementary Table 1.

Protein Extraction

Samples of 100–200 mg of tissue were immersed at a concentration of 200 mg/mL in a protein extraction solution containing 50 mM sodium phosphate buffer (pH 7.4) and Roche Complete Mini Protease Inhibitor Cocktail (Roche Applied Science, Indianapolis, IN). Tissue samples were homogenized on ice with a motor-driven tissue homogenizer (Fisher Tissue Miser, Thermo Fisher Scientific, Waltham, MA), followed by sonication on ice 10 times for 10 s each. The homogenates were centrifuged at 14 000 rpm in a benchtop centrifuge at 4 °C for 30 min, and the supernatants were filtered through 0.45-μm syringe filters. The filtrates (total soluble proteins) were used for subsequent heparin affinity chromatography and 2-D PAGE analysis. Protein concentrations were measured with the Bradford method using the Bio-Rad Protein Assay Kit (Bio-Rad, Hercules, CA) and bovine IgG as the standard on a μQuant plate reader (BioTek, Winooski, VT). All samples were stored at −80 °C until analysis.

Heparin Affinity Chromatography

Soluble protein extracts were fractionated on 5-mL HiTrap Heparin HP columns (GE Healthcare, Piscataway, NJ) using a GradiFrac system (GE Health-care). Typically, 12-mg protein samples were diluted with 50 mL of 10 mM sodium phosphate buffer at pH 7.4 (buffer A) and centrifuged at 10 000 rpm in a Sorvall SS-34 rotor (Thermo Fisher Scientific) at 4 °C for 20 min. The supernatant was loaded onto the heparin column at a rate of 2 mL/min. The column was washed with 75 mL of buffer A containing 20 mM NaCl to elute nonbinding proteins. Heparin-binding proteins were eluted using two-step gradients, 75 mL of 200 mM NaCl followed by 50 mL of 1 M NaCl (Figure 1A,B). Protein peaks were monitored by UV absorbance at 280 nm. Four protein pools were obtained from each tissue sample: total unfractionated extract (no heparin column), not heparin-binding (eluting with 20 mM NaCl wash), weakly heparin-binding (eluting with 200 mM NaCl), and strongly heparin-binding (eluting with 1 M NaCl). For 2-D PAGE or 2-D DIGE analysis, specimens were concentrated to 200 μL each at 4 °C using 10-kDa cutoff Amicon centrifugal filters (Millipore, Bedford, MA).

For Western blot validation, weakly heparin-binding fractions were obtained by batch purification. Heparin Sepharose (GE Healthcare) resin (0.2 mL) was equilibrated with buffer A containing 20 mM NaCl and mixed with tissue protein extract (1 mg of tissue in 1 mL of equilibration buffer) in a microcen-trifuge tube. After 10 min, the sample–resin mixture was centrifuged at 3000 rpm for 1 min. The supernatant was removed and 1 mL of equilibration buffer was added to the resin. The resuspended resin was centrifuged as above and the supernatant was removed. Then, the resin was mixed for 10 min with 1 mL of buffer A containing 200 mM NaCl. The resin was centrifuged and the supernatant containing eluted weakly heparin-binding proteins was saved. The buffer of the eluate was exchanged to buffer A using a 10-kDa cutoff Amicon centrifugal filter and concentrated to 30 μL for further experiments.

2-D PAGE

Protein samples (200 μg) from unfractionated total extracts, weakly heparin-binding, or strongly heparin-binding pools were analyzed by 2-D PAGE. Prior to electrophoresis, samples were cleaned with the ReadyPrep 2-D Cleanup Kit (Bio-Rad) and redissolved in 185 μL of ReadyPrep Rehydration/Sample Buffer (Bio-Rad). Protein samples were applied onto 11-cm IPG strips (pH 3–10, Bio-Rad), and the strips were rehydrated passively (without current) overnight in a Bio-Rad Protean IEF Focusing Tray. Proteins were separated in the strips by isoelectric focusing (IEF) using a Protean IEF Cell (Bio-Rad). After equilibration with SDS-PAGE Equilibration Buffers I and II (Bio-Rad), proteins were separated along the second dimension by SDS-PAGE using an 8–16% (m/v) gradient polyacrylamide Tris-HCl gel (Criterion Tris-HCl Gel, Bio-Rad). After electrophoresis, gels were fixed with 10% (v/v) ethanol and 7% (v/v) acetic acid for 30 min, and proteins were stained with fluorescent SYPRO Ruby (Bio-Rad) for 16 h. Stained gels were imaged with a Typhoon 9410 fluorescence scanner (GE Healthcare). Image analysis was carried out with the PD Quest 7.4.0 software (Bio-Rad). In the analysis, the intensity of each spot on a gel was normalized with respect to the total integrated optical fluorescence for that gel. The relative quantity of protein in a given spot was calculated as parts per million (ppm) of the total integrated optical fluorescence.

2-D DIGE

Proteomic profiles of total unfractionated extracts and heparin-binding fractions were compared by 2-D Difference Gel Electrophoresis (DIGE). Prior to analysis, protein samples were cleaned with the ReadyPrep 2-D Cleanup Kit (Bio-Rad) and resuspended in 28 μL of sample lysis buffer (30 mM Tris, 7 M urea, 2 M thiourea, and 4% (w/v) CHAPS, pH 8.5). The pH of the protein solutions was carefully adjusted to 8.5 with 50 mM NaOH by spotting 0.2-

μL samples onto a pH indicator strip. Paired protein samples (200 μg each) were labeled on ice for 30 min in the dark with 1 μL of 400 μM CyDye (GE Healthcare), for example, Cy5 for unfractionated total extracted proteins and Cy3 for heparin-binding fractions. The labeling reactions were stopped by incubation with 1 μL of 10 mM lysine for 10 min on ice in the dark. To the stopped reaction solution, 30 μL of sample buffer (8 M urea, 130 mM DTT, 4% (w/v) CHAPS, and 2% (v/v) Bio-Lyte 3/10 ampholyte (Bio-Rad)) was added. Pairs of labeled samples were pooled and the sample volume was adjusted to 185 μL with ReadyPrep Rehydration/Sample Buffer (Bio-Rad). The samples were mixed with 4 μL of 2-D SDS-PAGE Standard (Bio-Rad) and sequentially separated by IEF and SDS-PAGE as described above. Protein fluorescence images were obtained by imaging successively at 532 nm for Cy3 labeling and 635 nm for Cy5 labeling on a Typhoon 9410 scanner. Image analysis was performed as described above.

Protein Sequence Analysis by LC–MS/MS

Mass spectrometric sequencing was performed at the Taplin Biological Mass Spectrometry Facility of Harvard Medical School, Boston, MA. After 2-D PAGE gel image analysis, proteins that were differentially expressed in cancer tissue were selected for sequencing based on favorable positional separation on 2-D gels. Selected protein spots were excised and cut into approximately 1 mm^3 pieces. Gel pieces were then subjected to a modified in-gel trypsin digestion procedure.[8] Gel pieces were washed and dehydrated with acetonitrile for 10 min, followed by removal of acetonitrile. The gel pieces were then dried in a SpeedVac (Thermo Fisher Scientific, Waltham, MA). The gel pieces were rehydrated at 4 °C with 50 mM NH_4HCO_3 solution containing 12.5 ng/μL modified sequencing-grade trypsin (Promega, Madison, WI). After 45 min, the excess trypsin solution was removed and replaced with 50 mM NH_4HCO_3 solution to cover the gel pieces. Samples were incubated overnight at 37 °C. Tryptic peptides were then retrieved with NH_4HCO_3 solution, followed by one wash of the gel pieces with a solution containing 50% (v/v) acetonitrile and 5% (v/v) acetic acid. The extracts were dried in a SpeedVac and stored at 4 °C until analysis.

For analysis, the samples were reconstituted in 10 μL of HPLC solvent A (2.5% (v/v) acetonitrile, 0.1% (v/v) formic acid). A nanoscale reverse phase HPLC capillary column was created by packing 5-μm sized spherical C18 silica beads into a fused silica capillary (100 μm inner diameter, 12 cm length) with a flame-drawn tip.[9] After equilibration of the column, each sample was loaded via a Famos autosampler (LC Packings, San Francisco, CA). A gradient was formed and peptides were eluted at increasing concentrations of solvent B (97.5% (v/v) acetonitrile, 0.1% (v/v) formic acid).

As each peptide was eluted, it was subjected to electrospray ionization before entering into an LTQ linear ion trap mass spectrometer (Thermo Fisher Scientific). Eluting peptides were detected, isolated, and fragmented to produce a tandem mass spectrum of specific fragment ions for each peptide. Peak lists were generated with ExtractMS version 2 (rev. 11) (Thermo Fisher Scientific) using default parameters. Peptide sequences (and thus protein identities) were determined by matching the complete NCBI Human Protein Database (downloaded on 12/01/2006 from http://www.ncbi.nlm.nih.gov) without further restrictions containing 269 363 protein entries with the measured fragmentation pattern using the software program Sequest version 27 (rev. 12) (Thermo Fisher Scientific). For initial database searching and calculation of database match statistics, no enzyme cleavage specificity was considered to check independently whether database matches were indeed consistent with tryptic peptides. Cysteine *S*-carboxymethylation and methionine oxidation to methionine sulfoxide were accounted for as fixed and variable modifications, respectively. Mass tolerances for precursor and fragment ions were set to 2 and 1 Da, respectively. For acceptance of individual MS/MS spectra, peptides were required to be fully tryptic peptides with XCorr values of at least 1.5 (1^+ ion), 2.5 (2^+

ion), and 3.0 (3^+ ion), respectively. All data were manually inspected by an experienced mass spectrometrist, and only proteins with multiple peptide matches were considered confidently identified. When relevant, different isoforms or individual members of a protein family were identified based on the presence of peptide fragments unique to a particular isoform or family member. If such distinction was not possible, all candidates matching the measured peptides were reported.

Western Blotting

Mouse monoclonal antibodies specific for PSB7 (clone HN3), PRDX1 (clone 4b11-G10), and β-actin (clone C4) were purchased from Abcam (Cambridge, MA), Abnova (Taipei, Taiwan), and Santa Cruz Biotechnology (Santa Cruz, CA), respectively. Rabbit polyclonal IgG antibodies specific for SRP9 were purchased from ProteinTech (Chicago, IL). Further procedural details are given in Supporting Information.

Immunohistochemistry

Microtome sections (5 μm) from formalin-fixed and paraffin-embedded tissue blocks were mounted onto poly-L-lysine-coated glass slides. Routine diagnostic slides were stained with hematoxylin and eosin. Specific proteins were detected by peroxidase-DAB (diaminobenzidine) chemistry using the NovoLink Polymer Detection System (Vision BioSystems, Norwell, MA). Further procedural details are given in Supporting Information.

Results

Heparin Affinity Fractionation Enrichment (HAFE) of the Low-Abundance Proteome in Human Colorectal Mucosa

The enrichment of low-abundance proteins by heparin affinity chromatography was assessed using human colonic tissue protein extracts. Soluble protein extracts were prepared from normal or cancerous colonic mucosa and fractionated on heparin affinity columns into (*i*) nonbinding proteins (eluting with 20 mM NaCl), (*ii*) a weakly heparin-binding fraction (eluting with 200 mM NaCl), and (*iii*) a strongly heparin-binding fraction (eluting with 1 M NaCl). Figure 1A,B shows typical heparin affinity fractionation chromatograms. We then employed 2-D Difference Gel Electrophoresis (2-D DIGE) to compare the proteomic profiles of weakly and strongly binding proteins to those of unfractionated total protein extracts (Figure 1C,D). The overall protein signatures of heparin-binding protein fractions (green spots in Figure 1C,D) differed significantly from those of unfractionated samples (red spots). For example, albumin, an abundant protein in the unfractionated sample (red spot 1; identified by its molecular weight and p*I* position), was depleted in the heparin-binding fractions. In particular, the weakly heparin-binding fraction displayed a large number of enriched and newly visible proteins in the high p*I* range (green), possibly due to heparin-based selection for positive charge. Only few abundant proteins remained relatively unchanged by heparin affinity separation, as exemplified by the yellow spot 2. We then analyzed the gel images using the PD Quest software to quantitate depleted and enriched proteins in heparin-binding fractions relative to unfractionated total protein extracts. In the weakly binding fraction, 210 protein spots were enriched and 47 protein spots were partially or fully removed (enrichment bias, 210/47 = 4.5). In the strongly binding fraction, 216 protein spots were enriched and 14 protein spots were reduced (enrichment bias, 216/14 = 15.4). A greater than 2-fold absolute change (increase or decrease) in spot intensity was considered significant in this analysis. This result indicated that HAFE had the capability of preferentially enriching low-abundance proteins from tissue extracts. Thus, we hypothesized that HAFE could serve as a useful prefractionation tool for proteome analysis and discovery of novel biomarkers.

Next, we applied the HAFE technique to pairs of normal and cancerous mucosa from five patients who had undergone colectomy surgery for colon adenocarcinoma (Supplementary Table 1). Twelve milligrams each of soluble tissue protein extracts was fractionated. The average protein recovery rates in nonbinding, weakly, and strongly heparin-binding fractions from normal tissue were 47.1 ± 24.4% (5.7 ± 2.9 mg), 8.3 ± 2.1% (1.0 ± 0.3 mg) and 12.4 ± 14.5% (1.5 ± 1.7 mg), respectively. The corresponding recovery rates from adenocarcinoma tissue were 41.8 ± 8.8% (5.0 ± 1.1 mg), 10.6 ± 4.0% (1.3 ± 0.5 mg), and 21.4 ± 7.6% (2.6 ± 0.9 mg), respectively.

2-D PAGE Comparison of Heparin-Binding Fractions between Normal and Colon Cancer Tissue

The heparin-binding fractions isolated from normal and colorectal cancer samples were compared by 2-D PAGE. For this study, we analyzed 5 paired samples (patients CA1–5; see Supplementary Table 1 for clinical data) of weakly heparin-binding fractions and 4 paired samples (patients CA1–3 and CA5) of strongly heparin-binding fractions (Supplementary Figure 1). By computational 2-D gel image comparison, a total of 56 proteins were found to be differentially expressed between cancerous and normal tissue. Analysis of the weakly heparin-binding fractions revealed 42 differentially expressed protein spots, each exhibiting >2-fold relative abundance change (either increase or decrease) of the tumor to normal spot intensity ratio (SIR) in at least 3 patients and with >95% statistical significance (Student's *t* test). To better understand the effects of heparin prefractionation, we next asked how many spots would have been identified versus how many spots would have been missed in a 2-D gel analysis of unfractionated (i.e., not heparinenriched) extracts. To this end, we repeated the above analysis, now also including a 2-D gel data set from unfractionated total protein extracts obtained from patient CA2. Of the 42 spots, only 16 spots could be detected computationally when data from unfractionated extracts were included in the statistical analysis. Conversely, this means that 26 low-abundance, differentially expressed proteins were exclusively identified in the weakly heparin-binding fractions and thus would not have been discovered without HAFE prefractionation (Supplementary Figure 2). An analogous analysis was performed for the strongly heparin-binding fractions. Fourteen proteins were found to be differentially expressed (>2-fold change (either increase or decrease) in at least 3 patients and >95% statistical significance). After inclusion of a data set from unfractionated total protein extracts, 6 proteins were exclusively identified in the strongly heparin-binding fractions and thus would not have been discovered without HAFE prefractionation (Supplementary Figure 2). We hypothesized that those differentially expressed proteins that were exclusively detectable in heparin-prefractionated specimens may represent novel disease-associated proteins. Furthermore, such proteins would have likely been missed in previous studies using unfractionated samples alone. Hence, we decided to focus our attention on protein spots that were only detectable by analysis of HAFE fractions (32 protein spots, 26 from weakly and 6 from strongly heparin-binding fractions). Figure 2 shows 2-D gel images and spot intensity changes of the 32 proteins. Figure 2A depicts representative 2-D gels from weakly (left gel) and strongly (right gel) heparin-binding cancer tissue extracts, respectively. The positions of the 32 differentially expressed protein spots identified by HAFE analysis are indicated by numbers. To overcome intrinsic intra- and interspecimen variability associated with patient peculiarities and tissue heterogeneity, we required as the initial Boolean spot selection criteria (*i*) >2-fold abundance change of the SIR in at least 3 patients and (*ii*) >95% statistical significance by Student's *t* test as calculated by the PD Quest software. It is important to note that virtually all proteins selected by these criteria (Figure 2B,C) also showed the same qualitative trend (i.e., increase or decrease) for the remaining patients, albeit the changes were sometimes <2-fold or not statistically significant (Figure 2D).

Protein spots showing clear separation from surrounding spots, sufficient intensity, and consistent spot shape and size were chosen for identification by MS/MS sequencing. Four spots (numbered 7, 21, 23, and 25) were selected from the weakly binding fraction and 1 spot (numbered 32) was selected from the strongly binding fraction, respectively. Magnified gel views of the five spot locations from various patients are shown in Figure 2C. We identified the weakly heparin-binding proteins in spots 7, 21, 23, and 25 as proteasome subunit β type 7 (PSB7), argininosuccinate synthase (ASSY), hemoglobin α subunit (HBA), and peroxiredoxin-1 (PRDX1), respectively. The tightly heparin-binding protein in spot 32 corresponded to the signal recognition particle 9 kDa protein (SRP9) (Table 1 and Supplementary Table 2). The discovery of SRP9 illustrates the usefulness of heparin enrichment particularly well because the corresponding 2-D gel spot remained consistently undetectable in unfractionated extracts.

While all five proteins have been attributed various roles in oncogenesis, none has thus far been implicated in colorectal cancer. Thus, this is, to our knowledge, the first report demonstrating expression alterations of these proteins in human colorectal adenocarcinomas.

Validation of PSB7, PRDX1, and SRP9 Protein Overexpression in Colon Cancer by Western Blotting

We used Western blotting with monoclonal antibodies to validate the expression changes of PSB7, PRDX1, and SRP9 identified by 2-D PAGE analysis. Overall, 9 pairs of colon adenocarcinoma samples were analyzed. Furthermore, 15 pairs of lung adenocarcinoma samples were tested to study whether the observed protein expression changes were present in another common type of human adenocarcinoma. Figure 3 and Supplementary Figure 3 show the results of the Western blot validation for all available colon and lung cancer specimens. Unfractionated samples (Figure 3A,C and Supplementary Figure 3A), weakly heparin-binding fractions (Figure 3B,D,E), and strongly heparin-binding fractions (Supplementary Figure 3B) were examined. Omitted patient columns in individual blots indicate that no remaining specimen was available for the particular experiment. For comparison of protein expression levels between normal and cancer samples, the expression ratio (ER) between cancer and normal tissue was internally normalized with respect to β-actin protein expression levels for each pair of samples and calculated as $ER = (I_{PC}/I_{PN})/(I_{AC}/I_{AN})$, where I_{PC} and I_{PN} denote the measured intensities of the specific protein band (PSB7, PRDX1, or SRP9) for cancer or normal tissue, respectively, and I_{AC} and I_{AN} denote the measured intensities of the β-actin band for cancer and normal tissue, respectively. Consequently, $ER = 1$, $ER < 1$, and $ER < 1$ characterize overexpression in cancer, unchanged expression, and decreased expression in cancer, respectively.

In colon adenocarcinomas, the mean ERs (±standard deviation) for PSB7 in unfractionated and weakly heparin-binding tissue extracts were, respectively, 1.8 (±0.8) and 1.5 (±0.8). The second number may be a conservative estimate since the large value of ER = 22.8 for CA3 was not included in this analysis. For PRDX1, the corresponding mean ERs (±standard deviation) were 1.9 (±1.1) [unfractionated] and 2.1 (±1.1) [weakly heparin-binding], respectively. Again, the second number may be a conservative estimate since the large value of ER = 22.2 for CA4 was not included in this analysis. For SRP9, the mean ERs (±standard deviation) were 12.4 (±8.3) [unfractionated] and 73.6 (standard deviation omitted because of small sample size) [strongly heparin-binding], respectively.

Analysis of a control cohort of lung adenocarcinomas showed that the mean ERs (±standard deviation) for PSB7 in unfractionated and weakly heparin-binding tissue extracts were, respectively, 1.5 (±0.8) and 1.3 (±0.7). For PRDX1, the corresponding mean ERs (±standard deviation) were 2.1 (±1.4) [unfractionated] and 1.5 (±0.8) [weakly heparin-binding], respectively. For SRP9, the mean ERs (±standard deviation) were 4.8 (±3.1) [unfractionated]

and 1.6 (standard deviation omitted because of small sample size) [strongly heparin-binding], respectively.

2-D Western blot detection of PRDX1 revealed 4 isoforms in weakly heparin-binding fractions (Figure 3E). Individual 2-D Western SIRs for the 4 PRDX1 isoforms in patient CA4 were 2.5, 5.2, 9.3, and 37.0, respectively (Figure 3E; 4 spot pairs from left to right). The arrowheads indicate spots corresponding to spot 25 in Figure 2A, which was identified as PRDX1 by MS/MS sequencing (Table 1).

Localization of PSB7, PRDX1, and SRP9 Protein Overexpression in Colon Adenocarcinoma Tissue Sections

Our proteomic experiments, including the heparin-based enrichment for low-abundance proteins, had suggested increased expression of PSB7, PRDX1, and SRP9 proteins in primary human colon adenocarcinoma tissue. However, human cancer tissue is a complex, highly heterogeneous composite, typically including an admixture of *bona fide* neoplastic cancer cells, benign epithelial elements, mesenchymal stromal cells, blood and lymphatic vessels, nerve tissue, intercellular matrix elements, areas of necrosis or apoptosis, and numerous other components in varying proportions. While our proteomic approach provided a global look at the tissue as a whole, it did not permit to characterize protein expression distribution at a subtissue level. We therefore asked which of the tissue components expressed PSB7, PRDX1, or SRP9 proteins and whether overexpression could be directly demonstrated in tissue sections. To this end, we examined tissues from 2 patients (CA2 and CA7) by immunohistochemical techniques. Up-regulation of PSB7, PRDX1, and SRP9 was restricted to neoplastic colon cancer cells and was not identified in other components of primary tumor tissue, such as mesenchymal cells or vessels. At subcellular level, increased PSB7 levels were found both within cytoplasmic and nuclear compartments, while PRDX1 and SRP9 overexpression were predominantly cytoplasmic (Figures 4 and 5 and Supplementary Figure 4).

PSB7 was expressed at low levels in normal colonic mucosa (Figure 4A,B,E [left],F). Scattered mononuclear cells, mostly lymphocytes, also expressed PSB7. In contrast, PSB7 was found to be markedly up-regulated in both cytoplasm and nuclei of the malignant cells forming the abnormal and invasive adeno-carcinoma glands (Figure 4C,E [right],G,H). Furthermore, over-expression of PSB7 was also seen in carcinoma present within lymphatic vessels (Figure 4D).

Similarly, PRDX1 was detected at low levels in both normal colonic mucosa (Figure 5A [right],B,E [left],F) and scattered mononuclear cells, predominantly lymphocytes. However, invasive neoplastic glands displayed significantly increased, predominantly cytoplasmic PRDX1 (Figure 5A [left],C,E [right],G,H). Interestingly, a focus of colonic adenocarcinoma metastatic to the liver (patient CA2), which had been resected at the time of the colectomy procedure, also revealed markedly increased PRDX1 levels (Figure 5D), essentially indistinguishable from the primary tumor (Figure 5C).

While SRP9 expression was detectable in normal colonic (Supplementary Figure 4B,E,F) and scattered mononuclear cells in the lamina propria, overall levels were significantly higher in invasive carcinoma cells, both in the colon (Supplementary Figure 4A,C,G,H) and in a liver metastasis (Supplementary Figure 4D).

Analysis of sequential tissue sections from the same tissue blocks showed that PSB7, PRDX1, and SRP9 were overexpressed together by the same population of cancer cells, rather than distinctly by different subpopulations.

Discussion

In this study, we used a prefractionation technique, termed heparin affinity fractionation enrichment (HAFE), for preferential enrichment of the low-abundance primary human tissue proteome of surgical specimens. Conventional 2-D PAGE and direct MS/MS-based strategies have been challenged by the very large dynamic range of tissue protein concentrations, which spans approximately 10^5–10^{12}-fold differences. We demonstrated that polyanionic heparin can be used to enrich tissue proteome extracts for components that occur at relatively low abundance (Figure 1). On the basis of image analysis of 2-D DIGE experiments, we showed that through HAFE a richer and deeper view of the extractable proteome was achieved with spot enrichment biases of 450% and 1540% for weakly and strongly heparin-binding fractions, respectively (Figure 1C,D).

Next, we examined matched tissue pairs of human colonic adenocarcinoma and normal mucosa from patients who had undergone surgical colectomy procedures (Supplementary Table 1). Fifty-six protein spots were found to be differentially expressed between cancer and normal tissue (>2-fold relative change in at least 3 patients and >95% statistical significance). Of these, 42 were identified in weakly heparin-binding fractions and 14 in strongly heparin-binding fractions, respectively (Figure 2A,B, Supplementary Figure 1, and data not shown). Importantly, we demonstrated that omission of HAFE prefractionation would have failed to identify 62% (26/42) of weakly heparin-binding proteins and 43% (6/14) of strongly heparin-binding proteins. Thus, without HAFE, a total of 57% (32/56) of differentially expressed proteins would have remained undiscovered (Supplementary Figure 2).

We then focused on the 32 differentially regulated proteins identified exclusively by HAFE because we hypothesized that these proteins may have escaped previous investigation that did not employ HAFE methodology. Five particular protein spots were selected based on favorable 2-D electrophoretic separation behavior (Figure 2) and unambiguously identified by MS/MS sequence analysis (Table 1, Supplementary Table 2) as proteasome subunit β type 7 (PSB7), argininosuccinate synthase (ASSY), hemoglobin α subunit (HBA), peroxiredoxin-1 (PRDX1), and signal recognition particle 9 kDa protein (SRP9). Expression of 4 proteins (PSB7, ASSY, PRDX1, and SRP9) was increased in cancer tissue relative to normal control, while 1 protein (HBA) was decreased (Figure 2B,D).

There have been few proteomic studies of differentially expressed proteins in colorectal cancer tissue.[10–12] To our knowledge, however, none has used an enrichment strategy such as HAFE to augment the depth of the investigated proteome. Furthermore, none of the 5 proteins discovered in our study have been reported previously in colon cancer. This is consistent with our observation that, without HAFE, the sensitivity of unfractionated 2-D PAGE and MS/MS alone would have failed to identify the proteins as differentially expressed. Prefractionation by heparin affinity significantly enhanced visualization of the 5 proteins on the 2-D PAGE gels (Figure 2). Furthermore, it appears that heparin chromatography works not only by enriching heparin-binding proteins, but also by relatively depleting abundant proteins such as albumin (Figure 1C,D). The removal of abundant proteins increases the proportion of low-abundance proteins present in the same total quantity of sample, thus, enhancing sensitivity.

It is important to note that proteomic results embody a global look at heterogeneous intact, multifaceted tumor tissue, containing, besides neoplastic epithelial cancer cells, numerous other mucosal components, such as stroma, vessels, or smooth muscle. Therefore, increased or decreased tissue proteomic levels may not necessarily indicate altered expression within the cancer cells themselves but may, alternatively, be due to altered intra- or extracellular tissue microenvironment. We purposely chose this initial global approach to biomarker discovery over, for example, a microdissection-based approach because a whole tissue-based strategy

may be expected to capture *both* cancer cell *and* tissue milieu alterations (e.g., biological tumor-stroma microenvironmental changes including extracellular compositional alterations).

Along this line of thought, the observed decrease of HBA (and thus $\alpha_2\beta_2$ adult hemoglobin A) in tumor tissue is likely due to a relatively lower total blood content of tumor tissue compared to normal mucosa. Even though colon carcinomas are typically thought to possess increased microvascular density with respect to normal mucosa, they also contain an overproportionally increased solid epithelial mass component. Therefore, per mass unit of tissue, cancer tissue can be expected to contain less total hemoglobin than normal mucosa, contributing to the commonly hypoxic milieu of colon carcinoma.[13,14]

ASSY is a homotetrameric citrulline-aspartate ligase (EC 6.3.4.5) that catalyzes the ATP-dependent synthesis of arginine via argininosuccinate from citrulline and aspartate, a critical step in the urea cycle.[15] Genetic defects in ASSY cause auto-somal recessive citrullinemia. Arginine is the direct substrate for nitric oxide (NO) synthesis.[15] It is possible that in a hypoxic tumor microenvironment the rate of NO synthesis (and arginine depletion) would be increased to promote compensatory local vasodilatation. Consequently, an elevated arginine demand may cause concomitant up-regulation of ASSY under such conditions. Thus, ASSY overexpression in tumor tissue may be a biomarker of local tissue hypoxia.[16] Increased levels of ASSY have been observed in acute lymphocytic and myeloid leukemia cells [17,18] and ovarian surface epithelial carcinomas.[19]

Our subsequent work, however, focused on PSB7, PRDX1, and SRP9 because of the interesting biological functions of these proteins, the fact that these proteins had not been previously implicated in colon carcinogenesis, and the availability of reagents to validate our proteomic findings by methodologically independent approaches.

Up-regulation of PSB7, PRDX1, and SRP9 in cancer was validated by Western blotting using a tissue collection comprising 9 matched pairs of colon adenocarcinomas and a control cohort of 15 matched pairs of lung adenocarcinomas.

For colon adenocarcinomas, comparison of unfractionated and weakly (for PSB7 and PRDX1) or strongly (for SRP9) heparin-binding samples (Figure 3A–D and Supplementary Figure 3, left columns) showed that, while the ERs were not exactly of the same magnitudes on a patient by patient basis, they generally displayed a concordant trend. When directly comparing the data from 1-D Western blot experiments (Figure 3A–D and Supplementary Figure 3) to 2-D PAGE identification (Figure 2), several important experimental differences need to be considered: (*i*) One band in the 1-D Western represents the superposition intensity of usually several separate spots recognized by the same antibody on a 2-D gel, while only one particular spot on the 2-D PAGE gel was used for analysis (e.g., compare Figure 2A (spot 25) with Figure 3D (bands in CA4 lanes) and Figure 3E (4 spots each)); (*ii*) band/spot intensities in the Western blot experiments were enzymatically driven and chemiluminescence-based, whereas 2-D PAGE spot intensities were based on nonenzymatic SYPRO Ruby fluorescence dye staining, likely resulting in differences in sensitivity, response linearity, and dynamic range; and (*iii*) 1-D Western blot ERs were normalized relative to β-actin as an internal control to compensate for differences in gel loading, while 2-D PAGE analysis employed spot normalization with respect to total integrated 2-D gel fluorescence intensity. Furthermore, distinct spots on a 2-D gel originating from various isoforms of the same protein could exhibit differential behavior. For example, individual 2-D Western SIRs for 4 PRDX1 isoforms in patient CA4 were 2.5, 5.2, 9.3, and 37.0, respectively (Figure 3E; 4 spot pairs from left to right). The arrowheads in Figure 3E indicate spots corresponding to spot 25 in Figure 2A, which was identified as PRDX1 by MS/MS sequencing (Table 1). For comparison, the composite PRDX1 ER for patient CA4 from the corresponding 1-D Western blot experiment was 22.2 (Figure 3D), which falls within

the range of the 2-D Western data but does not capture the differential degree by which individual isoforms varied (range, 2.5–37.0-fold). Despite these differences, both Western blotting and 2-D PAGE results provided independent experimental evidence for robust up-regulation of PSB7, PRDX1, and SRP9 proteins in colon cancer tissue.

For lung adenocarcinomas, comparison of unfractionated and weakly heparin-binding samples on a patient by patient basis (Figure 3A–D, right column) showed a predominantly concordant trend for PRDX1 (i.e., both up or both down), while there was little concordance for PSB7. Concordance for SRP9 (Supplementary Figure 3, right column) could not be directly assessed because different sample sets had to be analyzed due to limited sample availability. PSB7 and PRDX1 ERs in the lung cancer cohort exhibited generally greater variability, and in addition, there were several patients who had decreased expression levels of PSB7 or PRDX1 in cancer tissue (ER < 1). This finding suggests that increased levels of PSB7 and PRDX1 may play a pathophysiologic role in or are a biomarker of colonic adenocarcinoma, while pulmonary adenocarcinoma, another very common human adenocarcinoma, may not share this property. 1-D Western blot analysis of SRP9 expression, in contrast, appears to suggest that this protein may also be up-regulated in pulmonary adenocarcinoma, a finding that awaits further study.

Finally, we demonstrated by immunohistochemistry on tissue sections that PSB7, PRDX1, and SRP9 protein up-regulation are localized to the neoplastic colon carcinoma cells, not other components of heterogeneous cancer tissue, such as stroma or vessels (Figures 4 and 5 and Supplementary Figure 4). PSB7 was increased in both cytoplasm and nucleus, while PRDX1 and SRP9 up-regulation was predominantly cytoplasmic. This is consistent with cell biological observations which have shown that PSB7 and the eukaryotic proteasome as a whole are found both in the cytoplasm and the nucleus,[20,21] while PRDX1 and SRP9 expression is predominantly cytoplasmic and, to a lesser degree, nuclear.[22–26] Interestingly, protein overexpression was retained in lymphatically spreading tumor cells (Figure 4D and Supplementary Figure 4A) and a hepatic metastasis (Figure 5D and Supplementary Figure 4D).

The biological relationship of PSB7, PRDX1, or SRP9 to heparin is currently not known, except that PRDX4, a homologous PRDX family member, can bind to heparin under reducing condition.[27] Several heparin-binding consensus peptide sequences have been proposed based on sequence alignments, including XBBXBX, XBBBXXBX and TXXBXXTBXXXTBB (B, basic residue; X, hydrophobic residue; T, turn).[28] The protein sequences of PSB7, PRDX1, and SRP9 were searched for these consensus motifs (Supplementary Table 2). PSB7 possesses two regions with repeated arrays of basic amino acids at ^{31}KRGYKLP-KVRK^{41} and ^{237}KKGTRLGRYRCEK^{249}. PRDX1 has two regions at ^{81}HFCHLAWVNTPKK^{93} and ^{185}KPDVQKSKEYFSKQK^{199}. Furthermore, SRP9 features such putative regions at ^{23}KARVV-LKYRH^{32} and ^{69}KKIEKFH^{75}. The calculated isoelectric points of PSB7, PRDX1, and SRP9 based on primary amino acid sequence are 7.58, 8.27, and 8.28, respectively, which is in keeping with their experimentally observed interaction with polyanionic heparin at physiologic pH. As would be expected, SRP9, which is the most basic of the three proteins, required the highest ionic strength for dissociation from heparin and was thus identified in the strongly heparin-binding fraction, while the other two were identified in the weakly heparin-binding fraction.

PSB7 is a component of the proteasome, a macromolecular machine integral to cellular proteolytic degradation capability.[29] The eukaryotic 20S proteasome is a cylinder-shaped assembly of four stacked rings of the general form $\alpha_7\beta_7\beta_7\alpha_7$.[30] The 20S particle is composed of 2 copies each of 14 different protein subunits (7 α subunits, PSA1–7; 7 β subunits, PSB1–7). PSB7 is part of a multicatalytic endopeptidase complex (composed of PSB5, PSB6, and PSB7). In response to interferon-γ signaling, the three subunits can be replaced by very homologous but different gene products, LMP7, LMP2, and MECL-1, respectively, forming

the so-called immunoproteasome.[31] At protein level, the regulation of PSB7 and MECL-1 appears to be reciprocal, that is, when PSB7 is down-regulated, MECL-1 is up-regulated and *vice versa.* Interestingly, down-regulation of LMP2, LMP10, and MECL-1 has been observed in human breast, colon, and lung cancers,[32–34] implying that their counterparts including PSB7 may be up-regulated compensatorily. It may be speculated that one selective advantage for cancer cells of shifting the pendulum away from the immunoproteasome is minimization of MHC class I immune recognition.[35,36] The functional role of PSB7 in cancer awaits further experimental investigation.

PRDX1 belongs to a family of thiol-specific peroxidases that reduce and detoxify a wide range of organic hydroperoxides such as H_2O_2 (37). PRDX1 has been studied in cancers and overexpression has been detected in oral squamous cell, thyroid, and pulmonary carcinomas.[38–43] Interestingly, transgenic mice lacking the *Prdx1* gene developed several cancers at increased frequency.[44] However, PRDX1 is not a conventional tumor suppressor because re-expression of peroxiredoxins in cancer cells fails to induce cell death.[45] Rather, peroxiredoxins may act as both gatekeepers of oxidative damage in normal tissue and promoters of survival of proliferating malignant cells that are exposed to increased metabolic oxidative stress.[41,42] PRDX3, another member of the PRDX family, has been found to protect malignant thymoma cells against hypoxia-induced H_2O_2 accumulation and apoptosis.[46] The precise functional roles and mechanisms of PRDX1 up-regulation in colon cancer will require further experimental study. Interestingly, at least 3 of the characterized differentially regulated proteins, that is, HBA, ASSY, and PRDX1, share the common theme of tissue hypoxia or hypoxia-related adaptation, a signature feature of malignancy.

SRP9 is part of the signal recognition particle (SRP), a hybrid protein-RNA complex that regulates translational targeting of membrane or secretory proteins to the endoplasmic reticulum.[47] The SRP can interact with the ribosome, recognize the nascent peptide chain, recruit the ribosome to the translocon, and initiate cotranslational protein sorting.[48–52] A heterodimeric complex of SRP9 and SRP14 bound to 5′ and 3′ terminal sequences of SRP RNA constitutes the SRP Alu domain which stalls translation elongation until the ribosome is properly positioned on the translocon.[53] As an RNA-binding protein, it may not be surprising that SRP9 was enriched in the strongly heparin-binding fractions (Figure 2A,C) because polysulfated heparin may mimic the anionic charge density of RNA. A recent gene array study identified up-regulation of SRP9 mRNA in hepatocellular carcinomas.[54] It is conceivable that the greater metabolic turnover in proliferating neoplastic cells necessitates increased ribosomal protein synthesis, in particular of membrane-associated proteins. Interestingly, anti-SRP autoantibodies have been detected in patients with paraneoplastic or autoimmune necrotizing myopathy.[55,56] The functional relationship between the SRP and malignancy awaits further study.

In summary, we describe the discovery of PSB7, PRDX1, and SRP9 protein up-regulation in human colon adenocarcinomas. The discovery was made possible by using a prefractionation approach for enhanced analysis of the low-abundance proteome of primary human surgical tissue specimens.

Supplementary Material

Refer to Web version on PubMed Central for supplementary material.

Acknowledgments

J.Y.W. acknowledges R01 grant support from the NIAID-NIH. We thank Dr. Steven Gygi and members of his laboratory at Harvard Medical School for advice and kind assistance with mass spectrometric experiments and data analysis.

References

1. American Cancer Society. Cancer Facts and Figures 2004. Atlanta, GA: http://www.cancer.org
2. Crawford NP, Colliver DW, Galandiuk S. Tumor markers and colorectal cancer: utility in management. J Surg Oncol 2003;84(4):239–48. [PubMed: 14756436]
3. Duffy MJ, van Dalen A, Haglund C, Hansson L, Klapdor R, Lamerz R, Nilsson O, Sturgeon C, Topolcan O. Clinical utility of biochemical markers in colorectal cancer: European Group on Tumour Markers (EGTM) guidelines. Eur J Cancer 2003;39(6):718–27. [PubMed: 12651195]
4. Ahmed N, Rice GE. Strategies for revealing lower abundance proteins in two-dimensional protein maps. J Chromatogr, B: Anal Technol Biomed Life Sci 2005 ;815(1–2):39–50.
5. Bianchini P, Osima B, Parma B, Nader HB, Dietrich CP. Pharmacological activities of heparins obtained from different tissues: enrichment of heparin fractions with high lipoprotein lipase, antihemolytic and anticoagulant activities by molecular sieving and antithrombin III affinity chromatography. J Pharmacol Exp Ther 1982;220(2):406–10. [PubMed: 7057400]
6. Shefcheck K, Yao X, Fenselau C. Fractionation of cytosolic proteins on an immobilized heparin column. Anal Chem 2003;75(7):1691–8. [PubMed: 12705604]
7. Tan HT, Zubaidah RM, Tan S, Hooi SC, Chung MC. 2-D DIGE analysis of butyrate-treated HCT-116 cells after enrichment with heparin affinity chromatography. J Proteome Res 2006;5(5):1098–106. [PubMed: 16674099]
8. Shevchenko A, Wilm M, Vorm O, Mann M. Mass spectrometric sequencing of proteins silver-stained polyacrylamide gels. Anal Chem 1996;68(5):850–8. [PubMed: 8779443]
9. Peng J, Gygi SP. Proteomics: the move to mixtures. J Mass Spectrom 2001;36(10):1083–91. [PubMed: 11747101]
10. Alfonso P, Nunez A, Madoz-Gurpide J, Lombardia L, Sanchez L, Casal JI. Proteomic expression analysis of colorectal cancer by two-dimensional differential gel electrophoresis. Proteomics 2005;5 (10):2602–11. [PubMed: 15924290]
11. Friedman DB, Hill S, Keller JW, Merchant NB, Levy SE, Coffey RJ, Caprioli RM. Proteome analysis of human colon cancer by two-dimensional difference gel electrophoresis and mass spectrometry. Proteomics 2004;4(3):793–811. [PubMed: 14997500]
12. Mazzanti R, Solazzo M, Fantappie O, Elfering S, Pantaleo P, Bechi P, Cianchi F, Ettl A, Giulivi C. Differential expression proteomics of human colon cancer. Am J Physiol Gastrointest Liver Physiol 2006;290(6):G1329–38. [PubMed: 16439467]
13. Vaupel P, Mayer A. Hypoxia and anemia: effects on tumor biology and treatment resistance. Transfus Clin Biol 2005;12(1):5–10. [PubMed: 15814285]
14. Yu JL, Coomber BL, Kerbel RS. A paradigm for therapy-induced microenvironmental changes in solid tumors leading to drug resistance. Differentiation 2002 ;70(9–10):599–609. [PubMed: 12492501]
15. Husson A, Brasse-Lagnel C, Fairand A, Renouf S, Lavoinne A. Argininosuccinate synthetase from the urea cycle to the citrulline-NO cycle. Eur J Biochem 2003;270(9):1887–99. [PubMed: 12709047]
16. Bizzoco E, Vannucchi MG, Faussone-Pellegrini MS. Transient ischemia increases neuronal nitric oxide synthase, argininosuccinate synthetase and argininosuccinate lyase co-expression in rat striatal neurons. Exp Neurol 2007;204(1):252–9. [PubMed: 17198704]
17. Ohno T, Kimura Y, Sakurada K, Sugimura K, Fujiyoshi T, Saheki T, Sonoda S, Azuma I. Argininosuccinate synthetase gene expression in leukemias: potential diagnostic marker for blastic crisis of chronic myelocytic leukemia. Leuk Res 1992;16(5):475–83. [PubMed: 1625473]
18. Sugimura K, Kimura T, Arakawa H, Ohno T, Wada Y, Kimura Y, Saheki T, Azuma I. Elevated argininosuccinate synthetase activity in adult T leukemia cell lines. Leuk Res 1990;14(10):931–4. [PubMed: 2259230]
19. Szlosarek PW, Grimshaw MJ, Wilbanks GD, Hagemann T, Wilson JL, Burke F, Stamp G, Balkwill FR. Aberrant regulation of argininosuccinate synthetase by TNF-alpha in human epithelial ovarian cancer. Int J Cancer 2007;121(1):6–11. [PubMed: 17354225]
20. Brooks P, Fuertes G, Murray RZ, Bose S, Knecht E, Rechsteiner MC, Hendil KB, Tanaka K, Dyson J, Rivett J. Subcellular localization of proteasomes and their regulatory complexes in mammalian cells. Biochem J 2000;346(Pt 1):155–61. [PubMed: 10657252]

21. Reits EA, Benham AM, Plougastel B, Neefjes J, Trowsdale J. Dynamics of proteasome distribution in living cells. EMBO J 1997;16(20):6087–94. [PubMed: 9321388]
22. Kang SW, Chae HZ, Seo MS, Kim K, Baines IC, Rhee SG. Mammalian peroxiredoxin isoforms can reduce hydrogen peroxide generated in response to growth factors and tumor necrosis factor-alpha. J Biol Chem 1998;273(11):6297–302. [PubMed: 9497357]
23. Kinnula VL, Lehtonen S, Sormunen R, Kaarteenaho-Wiik R, Kang SW, Rhee SG, Soini Y. Overexpression of peroxiredoxins I, II, III, V, and VI in malignant mesothelioma. J Pathol 2002;196 (3):316–23. [PubMed: 11857495]
24. Alavian CN, Politz JC, Lewandowski LB, Powers CM, Pederson T. Nuclear export of signal recognition particle RNA in mammalian cells. Biochem Biophys Res Commun 2004;313(2):351–5. [PubMed: 14684167]
25. Maity TS, Leonard CW, Rose MA, Fried HM, Weeks KM. Compartmentalization directs assembly of the signal recognition particle. Biochemistry 2006;45(50):14955–64. [PubMed: 17154533]
26. Politz JC, Yarovoi S, Kilroy SM, Gowda K, Zwieb C, Pederson T. Signal recognition particle components in the nucleolus. Proc Natl Acad Sci USA 2000;97(1):55–60. [PubMed: 10618370]
27. Okado-Matsumoto A, Matsumoto A, Fujii J, Taniguchi N. Peroxiredoxin IV is a secretable protein with heparin-binding properties under reduced conditions. J Biochem (Tokyo) 2000;127(3):493–501. [PubMed: 10731722]
28. Hileman RE, Fromm JR, Weiler JM, Linhardt RJ. Glycosaminoglycan-protein interactions: definition of consensus sites in glycosaminoglycan binding proteins. BioEssays 1998;20(2):156–67. [PubMed: 9631661]
29. Coux O, Tanaka K, Goldberg AL. Structure and functions of the 20S and 26S proteasomes. Annu Rev Biochem 1996;65:801–47. [PubMed: 8811196]
30. Voges D, Zwickl P, Baumeister W. The 26S proteasome: a molecular machine designed for controlled proteolysis. Annu Rev Biochem 1999;68:1015–68. [PubMed: 10872471]
31. Groettrup M, van den Broek M, Schwarz K, Macagno A, Khan S, de Giuli R, Schmidtke G. Structural plasticity of the proteasome and its function in antigen processing. Crit Rev Immunol 2001;21(4): 339–58. [PubMed: 11922078]
32. Gobbi G, Mirandola P, Micheloni C, Solenghi E, Sponzilli I, Artico M, Soda G, Zanelli G, Pelusi G, Fiorini T, Cocco L. Vitale MExpression of HLA class I antigen proteasome subunits LMP-2 LMP-10 in primary vs. metastatic breast carcinoma lesions. Int J Oncol 2004;25(6):1625–9. [PubMed: 15547699]
33. Johnsen A, France J, Sy MS, Harding CV. Down-regulation of the transporter for antigen presentation, proteasome subunits, and class I major histocompatibility complex in tumor cell lines. Cancer Res 1998;58(16):3660–7. [PubMed: 9721876]
34. Miyagi T, Tatsumi T, Takehara T, Kanto T, Kuzushita N, Sugimoto Y, Jinushi M, Kasahara A, Sasaki Y, Hori M, Hayashi N. Impaired expression of proteasome subunits and human leukocyte antigens class I in human colon cancer cells. J Gastroenterol Hepatol 2003;18(1):32–40. [PubMed: 12519221]
35. Cabrera CM, Jimenez P, Cabrera T, Esparza C, Ruiz-Cabello F, Garrido F. Total loss of MHC class I in colorectal tumors can be explained by two molecular pathways: beta2-microglobulin inactivation in MSI-positive tumors and LMP7/TAP2 downregulation in MSI-negative tumors. Tissue Antigens 2003;61(3):211–9. [PubMed: 12694570]
36. Mehling M, Simon P, Mittelbronn M, Meyermann R, Ferrone S, Weller M, Wiendl H. WHO grade associated downregulation of MHC class I antigen-processing machinery components in human astrocytomas: does it reflect a potential immune escape mechanism. Acta Neuropathol 2007;114(2): 111–9. [PubMed: 17541610]
37. Wood ZA, Schroder E, Robin Harris J, Poole LB. Structure, mechanism and regulation of peroxiredoxins. Trends Biochem Sci 2003;28(1):32–40. [PubMed: 12517450]
38. Yanagawa T, Ishikawa T, Ishii T, Tabuchi K, Iwasa S, Bannai S, Omura K, Suzuki H, Yoshida H. Peroxiredoxin I expression in human thyroid tumors. Cancer Lett 1999;145(1–2):127–32. [PubMed: 10530780]
39. Yanagawa T, Iwasa S, Ishii T, Tabuchi K, Yusa H, Onizawa K, Omura K, Harada H, Suzuki H, Yoshida H. Peroxiredoxin I expression in oral cancer: a potential new tumor marker. Cancer Lett 2000;156(1):27–35. [PubMed: 10840156]

40. Li R, Wang H, Bekele BN, Yin Z, Caraway NP, Katz RL, Stass SA, Jiang F. Identification of putative oncogenes in lung adenocarcinoma by a comprehensive functional genomic approach. Oncogene 2006;25(18):2628–35. [PubMed: 16369491]
41. Kim YJ, Lee WS, Ip C, Chae HZ, Park EM, Park YM. Prx1 suppresses radiation-induced c-Jun NH2-terminal kinase signaling in lung cancer cells through interaction with the glutathione S-transferase Pi/c-Jun NH2-terminal kinase complex. Cancer Res 2006;66(14):7136–42. [PubMed: 16849559]
42. Kim YJ, Ahn JY, Liang P, Ip C, Zhang Y, Park YM. Human prx1 gene is a target of Nrf2 and is up-regulated by hypoxia/reoxygenation: implication to tumor biology. Cancer Res 2007;67(2):546–54. [PubMed: 17234762]
43. Kim JH, Bogner PN, Ramnath N, Park Y, Yu J, Park YM. Elevated peroxiredoxin 1, but not NF-E2-related factor 2, is an independent prognostic factor for disease recurrence and reduced survival in stage I non-small cell lung cancer. Clin Cancer Res 2007;13(13):3875–82. [PubMed: 17606720]
44. Neumann CA, Krause DS, Carman CV, Das S, Dubey DP, Abraham JL, Bronson RT, Fujiwara Y, Orkin SH, Van Etten RA. Essential role for the peroxiredoxin Prdx1 in erythrocyte antioxidant defence and tumour suppression. Nature 2003;424(6948):561–5. [PubMed: 12891360]
45. Neumann CA, Fang Q. Are peroxiredoxins tumor suppressors. Curr Opin Pharmacol 2007;7(4):375–80. [PubMed: 17616437]
46. Nonn L, Berggren M, Powis G. Increased expression of mitochondrial peroxiredoxin-3 (thioredoxin peroxidase-2) protects cancer cells against hypoxia and drug-induced hydrogen peroxide-dependent apoptosis. Mol Cancer Res 2003;1(9):682–9. [PubMed: 12861054]
47. Hsu K, Chang DY, Maraia RJ. Human signal recognition particle (SRP) Alu-associated protein also binds Alu interspersed repeat sequence RNAs. Characterization of human SRP9. J Biol Chem 1995;270(17):10179–86. [PubMed: 7730321]
48. Egea PF, Stroud RM, Walter P. Targeting proteins to membranes: structure of the signal recognition particle. Curr Opin Struct Biol 2005;15(2):213–20. [PubMed: 15837181]
49. Halic M, Becker T, Pool MR, Spahn CM, Grassucci RA, Frank J, Beckmann R. Structure of the signal recognition particle interacting with the elongation-arrested ribosome. Nature 2004;427(6977):808–14. [PubMed: 14985753]
50. Halic M, Beckmann R. The signal recognition particle and its interactions during protein targeting. Curr Opin Struct Biol 2005;15(1):116–25. [PubMed: 15718142]
51. Halic M, Blau M, Becker T, Mielke T, Pool MR, Wild K, Sinning I, Beckmann R. Following the signal sequence from ribosomal tunnel exit to signal recognition particle. Nature 2006;444(7118):507–11. [PubMed: 17086193]
52. Halic M, Gartmann M, Schlenker O, Mielke T, Pool MR, Sinning I, Beckmann R. Signal recognition particle receptor exposes the ribosomal translocon binding site. Science 2006;312(5774):745–7. [PubMed: 16675701]
53. Weichenrieder O, Wild K, Strub K, Cusack S. Structure and assembly of the Alu domain of the mammalian signal recognition particle. Nature 2000;408(6809):167–73. [PubMed: 11089964]
54. Liu Y, Zhu X, Zhu J, Liao S, Tang Q, Liu K, Guan X, Zhang J, Feng Z. Identification of differential expression of genes in hepatocellular carcinoma by suppression subtractive hybridization combined cDNA microarray. Oncol Rep 2007;18(4):943–51. [PubMed: 17786358]
55. Sampson JB, Smith SM, Smith AG, Singleton JR, Chin S, Pestronk A, Flanigan KM. Paraneoplastic myopathy: response to intravenous immunoglobulin. Neuromusc Disord 2007;17(5):404–8. [PubMed: 17336069]
56. Hengstman GJ, ter Laak HJ, Vree Egberts WT, Lundberg IE, Moutsopoulos HM, Vencovsky J, Doria A, Mosca M, van Venrooij WJ, van Engelen BG. Anti-signal recognition particle autoantibodies: marker of a necrotising myopathy. Ann Rheum Dis 2006;65(12):1635–8. [PubMed: 16679430]
57. Compton CC, Greene FL. The staging of colorectal cancer: 2004 and beyond. CA Cancer J Clin 2004;54(6):295–308. [PubMed: 15537574]
58. Lababede O, Meziane MA, Rice TW. TNM staging of lung cancer: a quick reference chart. Chest 1999;115(1):233–5. [PubMed: 9925089]

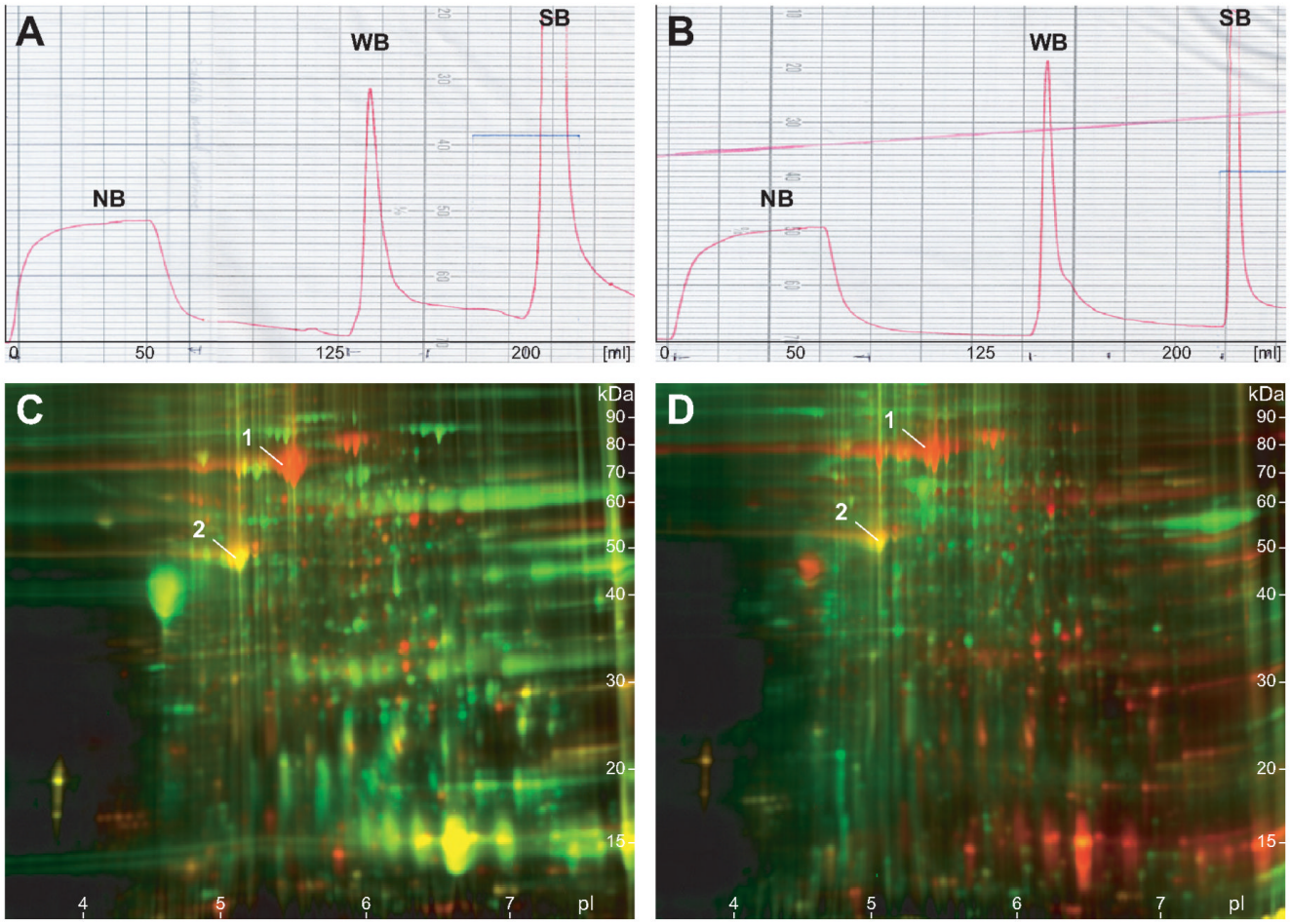

Figure 1.

Heparin affinity fractionation chromatograms and 2-D DIGE analysis of heparin affinity enrichment. (A and B) Heparin affinity chromatograms of normal (A) and adenocarcinoma (B) tissue samples from patient CA2. Samples (12 mg) of soluble total proteins extracted from colonic mucosa were loaded onto a HiTrap Heparin HP column (5 mL bed volume). Abscissa and ordinate of the chromatograms denote column elution volume and UV absorbance at 280 nm, respectively. The first broad peak corresponds to nonbinding proteins (NB). The two sharp peaks represent weakly (WB) and strongly heparin-binding (SB) proteins eluting at 200 mM and 1 M NaCl, respectively. The chromatographic profiles of normal versus disease or between different patients were overall similar to each other and reproducible without significant changes. For 2-D PAGE analysis, the peak fractions were collected and pooled to minimize small variations between runs. (C and D) Assessment of heparin affinity fractionation enrichment by 2-D Difference Gel Electrophoresis (DIGE). Total soluble proteins extracted from normal colonic mucosa (patient CA3) were separated by heparin affinity as above. Unfractionated total proteins (200 μg) were labeled with the Cy5 dye (red), while heparin-binding proteins (200 μg) were labeled with the Cy3 dye (green). Preferentially enriched proteins in weakly (C) and strongly (D) heparin-binding fractions are shown in green in the overlay images, while relatively depleted, originally abundant proteins are highlighted in red. Yellow spots identify few proteins whose abundance remains unchanged by fractionation. Note the significant increase in the number of resolved weak green spots over strong red spots, indicating the efficiency of low-abundance proteome enrichment by heparin fractionation.

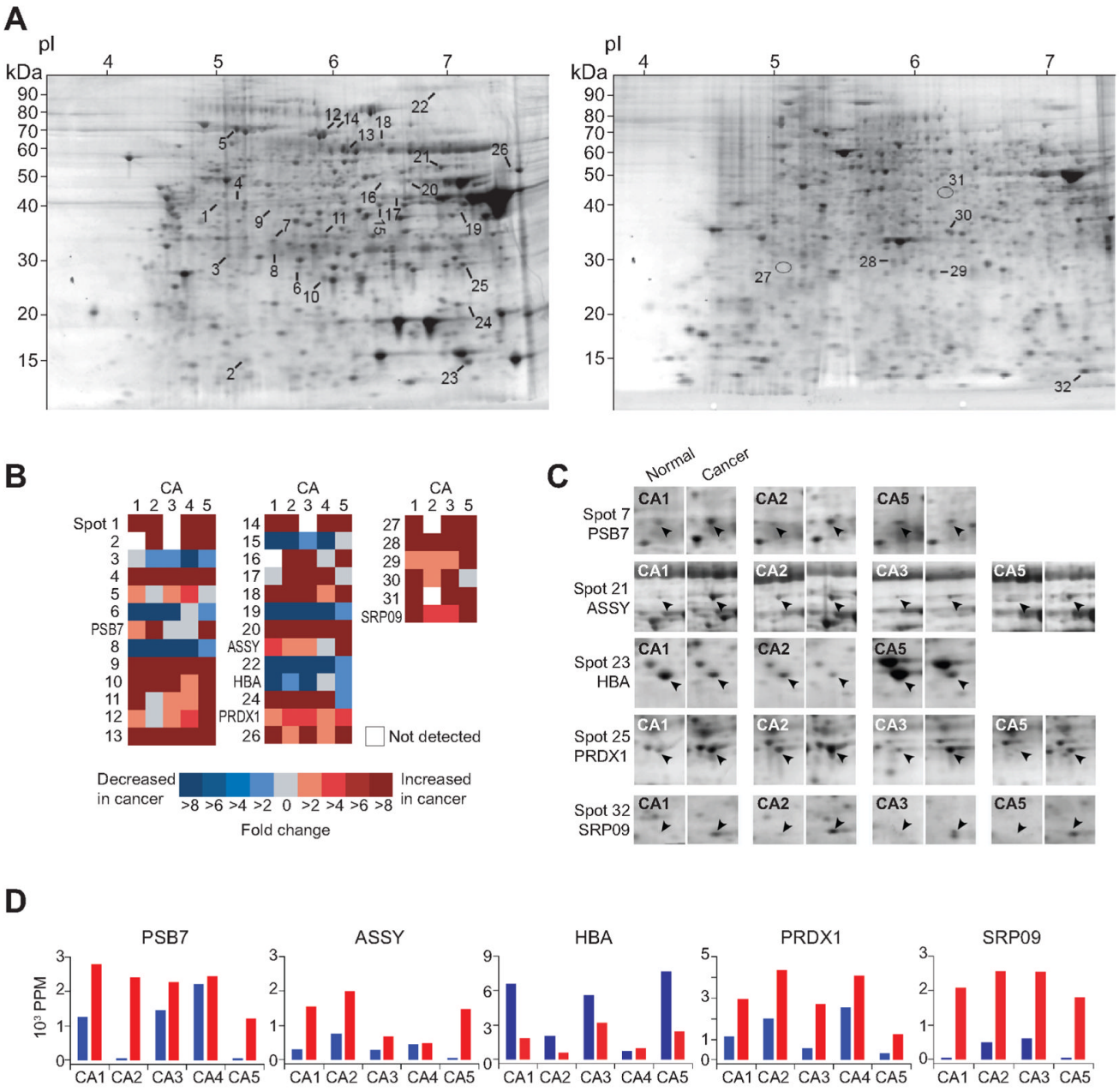

Figure 2.

Differentially expressed proteins in human colorectal cancer tissues. (A) Representative 2-D PAGE gel images of weakly (left; patient CA5) and strongly (right; patient CA2) heparin-binding proteins extracted from cancer tissues. Thirty-two spots showing >2-fold relative change (either increase or decrease) in at least 3 patients with >95% statistical significance are labeled with numbers. Five protein spots (numbered 7, 21, 23, 25, and 32) showing clear separation from surrounding spots, sufficient intensity, and consistent spot shape and size were chosen for identification by MS/MS sequencing. The two ellipses indicate spot positions which were identified from other gels, but are very weak on this gel. (B) Heat map representation of protein expression level changes in colorectal cancer tissues. The columns correspond to patients CA1–5 (spots 1–26; weakly heparin-binding proteins) or CA1–3 and CA5 (spots 27–32; strongly heparin-binding proteins). Each cell is color-coded for fold increase (shades of

red) or fold decrease (shades of blue) in cancer compared to matched normal mucosa. Gray cells indicate that the spot intensities in normal and cancer specimens were approximately equal. Blank cells denote absence of spots in the respective gels. (C) Magnified paired views of the sequenced protein spots (arrowheads) from various patient samples (left, normal mucosa; right, cancer). The gel details shown fulfill the Boolean selection criteria, i.e., >2-fold change in at least 3 patients and >95% statistical significance. (D) Bar graph representations of spot intensities for PSB7, ASSY, HBA, PRDX1, and SRP9 proteins. Blue and red bars denote normal mucosa and cancer tissue, respectively. Abscissae are labeled by patient number. Ordinates express the relative amount of protein in a given spot as parts per million (ppm) of the total integrated gel fluorescence.

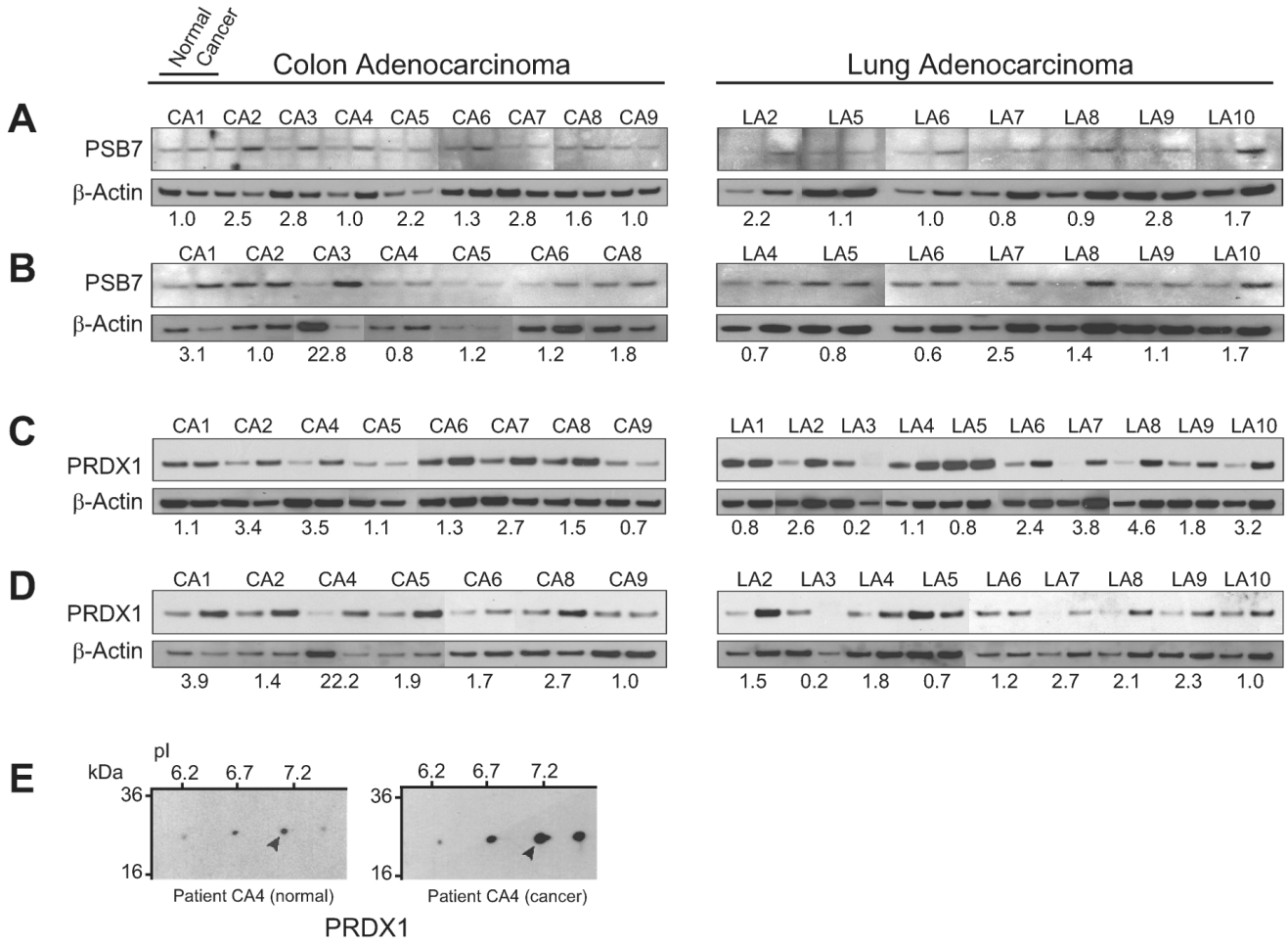

Figure 3.

Validation of PSB7 and PRDX1 overexpression by Western blotting. (A–D) 1-D Western blot analysis of PSB7 and PRDX1 expression in normal and cancer tissue. Results for unfractionated total soluble tissue extracts (A and C) and weakly heparin-binding fractions (B and D) are shown. For comparison of protein expression levels between normal and cancer samples, the expression ratio (ER) between cancer and normal tissue was calculated and normalized with respect to β-actin protein expression levels for each pair of samples (shown as numbers below the gel images; see text). Consequently, ER > 1, ER = 1, and ER < 1 characterize overexpression in cancer, unchanged expression, and decreased expression in cancer, respectively. (E) 2-D Western blot detection of 4 PRDX1 isoforms in weakly heparin-binding fractions from patient CA4 (left gel, normal; right gel, cancer). The arrowheads denote the spot location corresponding to spot 25 in Figure 2A, which was identified as PRDX1 by MS/MS sequencing. Abbreviations: CA, colon adenocarcinoma; LA, lung adenocarcinoma.

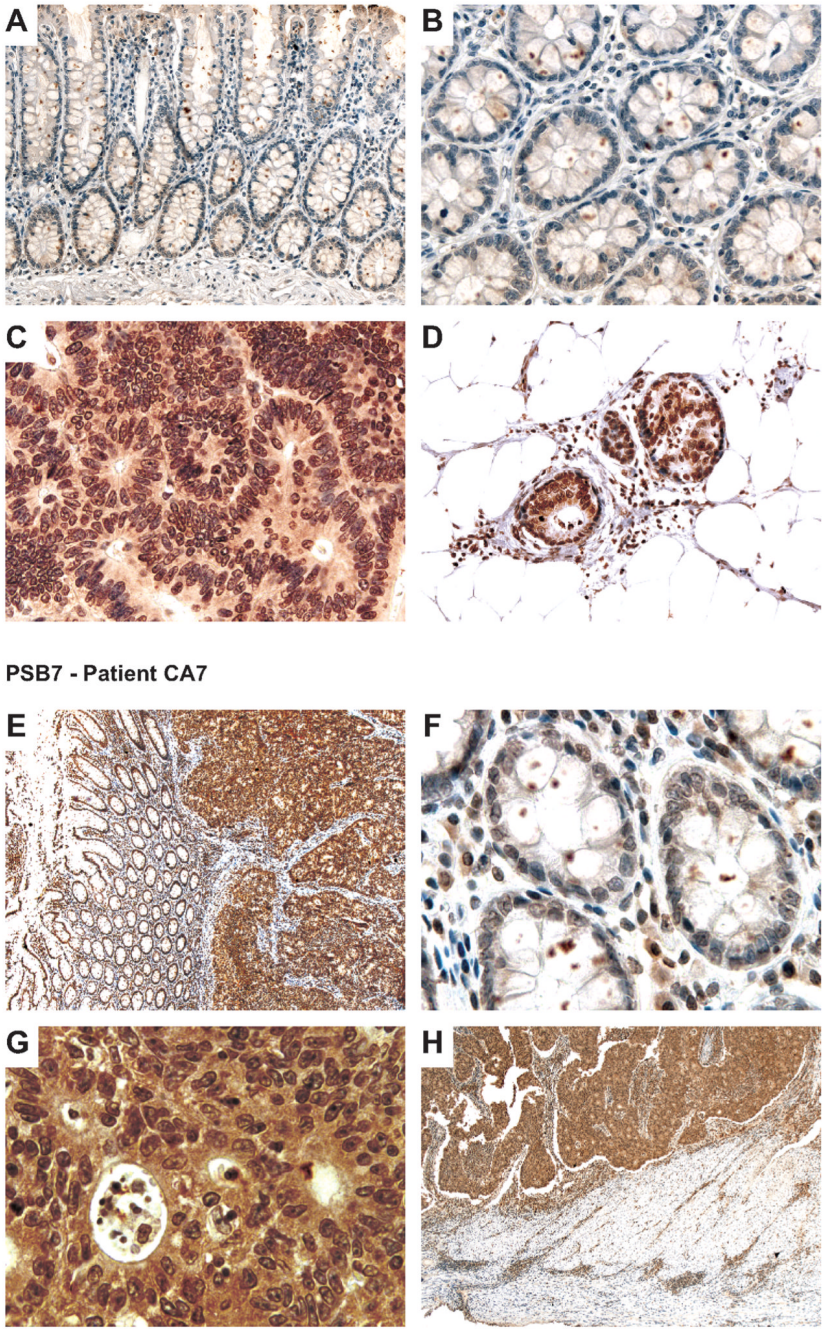

Figure 4.

Immunohistochemical localization of PSB7 expression in colon adenocarcinomas. The tissue sections shown are from patients CA2 (A–D) and CA7 (E–H). PSB7 expression was visualized by immunohistochemistry using 5-μm paraffin-embedded tissue sections. Presence of the specific protein is indicated by the amount of brown staining. Nuclei were counterstained with hematoxylin for visualization purposes. (A and B) Normal colonic mucosa with low levels of PSB7 expression. (C) Markedly increased cytoplasmic and nuclear PSB7 expression in the patient's adenocarcinoma. (D) PSB7 expression in carcinoma present in pericolonic lymphatic vessels; note the surrounding adipose tissue. (E) Normal mucosa (left) with low expression of PSB7 undermined by invasive adenocarcinoma in the submucosa featuring high levels of

PSB7. (F) Normal mucosal crypts and lamina propria with low levels of PSB7 expression. (G and H) Adenocarcinoma with high levels of PSB7 invading the muscularis propria (H, bottom); note the rim of PSB7-expressing lymphocytes at the invasive front of the tumor (H). Original magnifications: (A) 100×; (B) 400×; (C) 400×; (D) 200×; (E) 50×; (F) 630×; (G) 630×; (H) 50×.

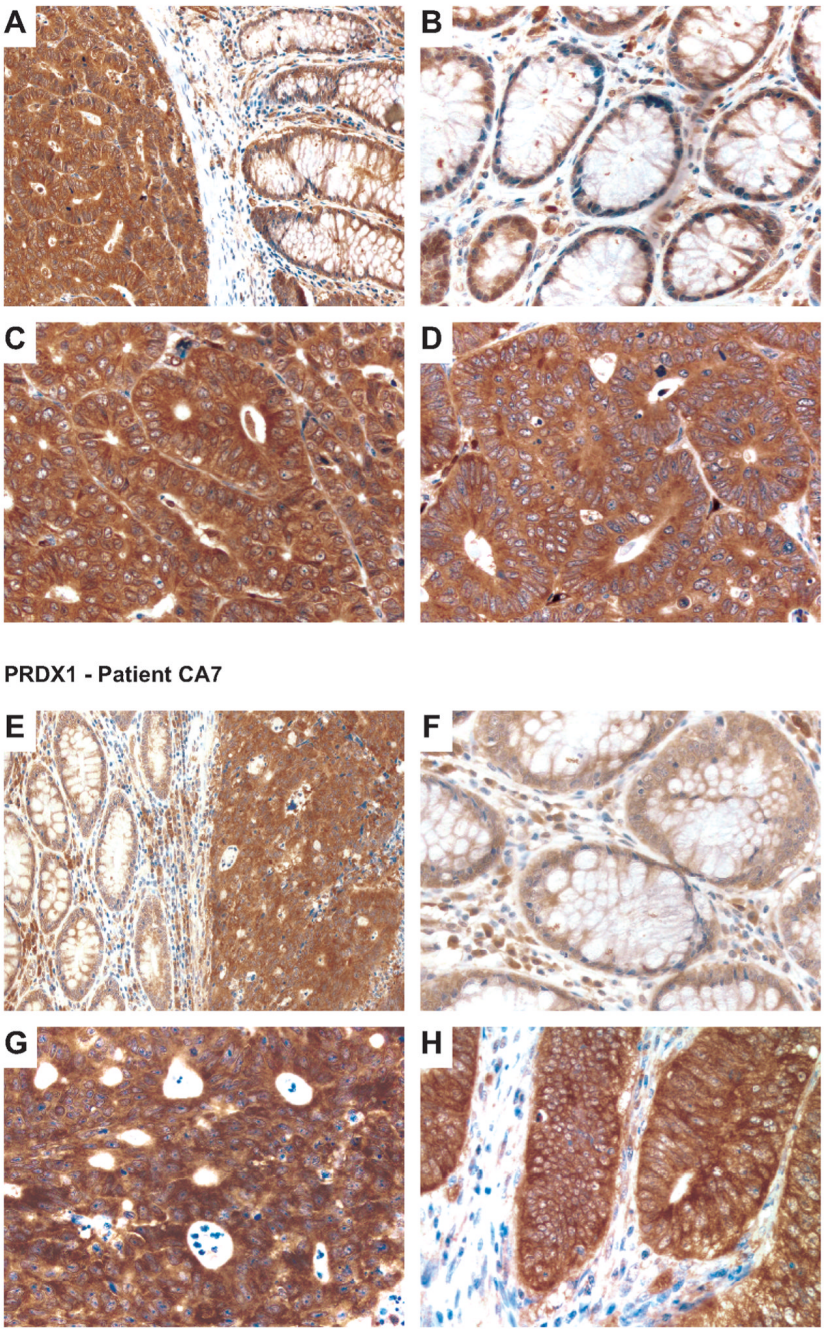

Figure 5.

Immunohistochemical localization of PRDX1 expression in colon adenocarcinomas. The tissue sections shown are from patients CA2 (A–D) and CA7 (E–H). PRDX1 expression was visualized by immunohistochemistry using 5-μm paraffin-embedded tissue sections. Presence of the specific protein is indicated by the amount of brown staining. Nuclei were counterstained with hematoxylin for visualization purposes. (A–C) Normal mucosa and lamina propria (A, right; B) and invasive adenocarcinoma (A, left; C) illustrating up-regulation of PRDX1 protein in the carcinoma. (D) Liver metastasis of the patient's primary colonic carcinoma featuring marked PRDX1 overexpression and overall morphology essentially indistinguishable from the primary tumor. Note that no normal liver parenchyma is present in the field shown. (E–H)

Normal mucosa and lamina propria (E, left; F) and invasive adenocarcinoma (E, right; G and H) demonstrating a relative increase of PRDX1 protein in the carcinoma. Original magnifications: (A) 200×; (B) 400×; (C) 400×; (D) 400×; (E) 200×; (F) 400×; (G) 400×; (H) 200×.

Table 1

Differentially Expressed Proteins Identified in Weakly and Strongly Heparin-Binding Fractions by MS/MS (Tandem) Mass Spectrometry[a]

Spot	SIR	Expt MW/pI	Theor. MW/pI	MS/MS Coverage	Identity	UniProtKB Entry
7	6.1	32.8/5.52	29.8/7.58	152/277(54.9%)	Proteasome subunit β type 7 (PSB7)	Q99436
21	4.5	53.6/6.96	46.5/8.08	247/412(60.0%)	Argininosuccinate synthase (ASSY)	P00966
23	0.22	14.4/7.20	15.1/8.73	67/141 (47.5%)	Hemoglobin α subunit (HBA)	P69905
25	3.3	28.1/7.18	22.1/8.27	139/199(69.8%)	Peroxiredoxin- 1 (PRDX1)	Q06830
32	6.3	12.5/7.48	10.0/8.28	37/85 (43.5%)	Signal recognition particle 9 kDa protein (SRP9)	P49458

[a]SIR, cancer to normal spot intensity ratio (>1.0, increased expression in cancer; 1.0, unchanged expression; <1.0, decreased expression in cancer). Spot 32 was identified in the strongly heparin-binding fractions; all other spots were identified in the weakly heparin-binding fractions. Experimental and theoretical molecular weights (MW in kDa) and isoelectric points (p*I*) were determined from referenced 2-D gel spot positions and database sequence entries, respectively. Note that the theoretical values do not account for potential post-translational modification. MS/MS coverage denotes the number of amino acids in positive peptide mass matches relative to the total number of amino acids of the mature protein. 10, 23, 4, 14, and 4 distinct tryptic peptide fragment matches could be assigned for PSB7, ASSY, HBA, PRDX1, and SRP9, respectively.